Cellular Signalling 32 (2017) 124–132

Contents lists available at ScienceDirect

Cellular Signalling

journal homepage: www.elsevier.com/locate/cellsig

# Antiproliferative effects of Bortezomib in endothelial cells transformed by viral G protein-coupled receptor associated to Kaposi's sarcoma

SuaresA [a], Mori Sequeiros GarciaM [b], PazC [b], González-PardoV [a,*]

[a] Institute of Science Biology and Biomedical Research (INBIOSUR, UNS-CONICET), Department of Biology, Biochemistry and Pharmacy, Universidad Nacional del Sur, San Juan 670, 8000 Bahia Blanca, Argentina
[b] Institute for Biomedical Research (INBIOMED, UBA-CONICET), Department of Biochemistry, School of Medicine, Universidad de Buenos Aires, Paraguay 2155, C1121ABG Buenos Aires, Argentina

ARTICLE INFO

*Article history:*
Received 1 November 2016
Received in revised form 30 January 2017
Accepted 30 January 2017
Available online 01 February 2017

*Keywords:*
Bortezomib
MKP-3
ERK 1/2
FOXO1
vGPCR

ABSTRACT

The Kaposi's Sarcoma-associated Herpes virus G Protein-Coupled Receptor (vGPCR) is a key molecule in the pathogenesis of Kaposi Sarcoma. We have previously demonstrated that the proteasome inhibitor Bortezomib inhibits NF-κB pathway, which is required for tumor maintenance in endothelial cells that express vGPCR (vGPCR cells). In this work, we further investigated Bortezomib anti-proliferative mechanism of action. We demonstrated that Bortezomib decreases vGPCR cell number in a dose-dependent manner and induces cell morphology changes. Bortezomib decreases ERK1/2 phosphorylation whereas induces the accumulation of MKP-3 – a specific ERK1/2 MAP kinase phosphatase – in time and concentration dependent manner (1.5–32 h; 0.25–1 nM). The transcription factor FOXO1 is activated by dephosphorylation and regulates p21 expression. Here, we demonstrated that Bortezomib increases FOXO1 protein and decreases its phosphorylation in a concentration dependent manner (0.25–1 nM). Bortezomib (0.5 nM, 24 h) also increase nuclear FOXO1 protein, in line with FOXO1 dephosphorylation induced by the drug. Consistent with FOXO1 dephosphorylation/activation, p21 mRNA expression is increased by Bortezomib in a MKP-3-dependent way. Bortezomib (0.5 nM, 24 h) also decreases VEGF, an ERK1/2 -dependent effect. It is concluded that in vGPCR cells, Bortezomib decreases ERK1/2 and FOXO1 phosphorylation through MKP-3 accumulation, leading ERK1/2 deactivation and FOXO1 activation respectively and, consequently, to cell proliferation inhibition, p21 induction and VEGF repression. Taken together, all these events contribute to the anti-tumoral effect of Bortezomib.



## 1. Introduction

Human Herpesvirus-8 (HHV-8) or Kaposi's Sarcoma-Associated Herpesvirus (KSHV) is a member of the gamma-herpesvirus family. KSHV is unique among the viruses associated with human cancer and was first isolated from human AIDS-Kaposi's sarcoma (KS) lesions by Chang and Moore [1]. KSHV virally encoded G protein-coupled receptor (vGPCR) is a constitutively active lytic phase protein with significant homology to the human interleukin-8 receptor [2,3]. Transgenic expression of vGPCR induces angiogenic lesions similar to human Kaposi sarcoma lesions [4,5], which are heterogeneous and contain endothelial-derived spindle cells as well as multiple inflammatory and mesenchymal cells. vGPCR oncogenic expression in endothelial cells may contribute to sarcomagenesis both through complex signaling network activation including the NF-κB and Akt-mTOR pathways and multiple Rho GTPases and mitogen-activated protein kinases (MAPKs), and the concomitant expression of potent proangiogenic, proinflammatory and chemo-attractant factors [2]. As persistent vGPCR expression and activity are required for tumor maintenance [6], this receptor and its corresponding signaling pathways may represent suitable candidates for KS treatment [7].

The dipeptide boronic acid analog VELCADE™ (Bortezomib; formerly known as PS-341, LDP-341 and MLM341) is a potent and selective inhibitor of the proteasome, a multicatalytic enzyme that mediates many cellular regulatory signals by degrading regulatory proteins or their inhibitors [8]. Bortezomib at low nanomolar concentration is sufficient to inhibit the activation of NF-κB [9]. The effects of Bortezomib have been demonstrated in a broad range of human tumor cell types in vitro [10,11] and in vivo against a variety of malignancies, including myeloma, chronic lymphocytic leukemia, prostate cancer, pancreatic cancer, and colon cancer [8,12]. Supporting these effects, we have recently reported that Bortezomib decreases nuclear activity of NF-κB [13] and induces apoptosis in endothelial cells expressing vGPCR [14].

*Abbreviations:* vGPCR, Kaposi's Sarcoma-associated Herpes virus G Protein-Coupled Receptor; NF-κB, nuclear factor kappa B; MAPK, mitogen-activated protein kinase; MKP-3, mitogen-activated protein (MAP) kinase-phosphatase-3; FOXO1, Forkhead box protein O1; VEGF, vascular endothelial growth factor; KSHV, Kaposi's Sarcoma-Associated Herpesvirus; HHV-8, Human Herpesvirus-8; KS, Kaposi sarcoma.

* Corresponding author at: Departamento Biología Bioquímica & Farmacia, INBIOSUR, CONICET, Universidad Nacional del Sur, San Juan 670, 8000 Bahía Blanca, Argentina.
*E-mail address:* vgpardo@criba.edu.ar (V. González-Pardo).

http://dx.doi.org/10.1016/j.cellsig.2017.01.025
0898-6568/

In endothelial cells expressing vGPCR, MAPK activity and the regulation of many MAPK-dependent signaling pathways seem to be relevant to tumoral phenotype maintenance. As MAPK activation is dependent on phosphorylation in specific threonine and tyrosine residues, the magnitude and duration of MAPK activity -and, consequently, all MAPK-dependents processes- are linked to the action of phosphatases capable of dephosphorylating and inactivating them.

MAPK phosphatases (MKPs) are dual specificity (threonine and tyrosine) phosphatases (DUSPs) involved in MAPK regulation [15–17]. MKP family members differ in their subcellular localization, tissue-specific expression, inducibility by various types of signals, and selectivity for dephosphorylating specific MAPKs. MKP-1, -2 and -3 are well characterized members of the MKP family. MKP-1 and MKP-2 (or DUSP1 and DUSP4) are nucleus-localized phosphatases capable of dephosphorylating all members of the three subgroups of MAPK (extracellular-regulated kinases or ERKs, c-Jun NH2-terminal protein kinases, or JNK1/2 and p38 proteins) and induced by several types of stimulus, but exhibiting different kinetics. In contrast, MKP-3 (or DUSP6) is a cytoplasmic enzyme induced by different proliferative stimuli -but not by environmental stress-and is characterized as a highly specific phosphatase for attenuating ERK1/2 signaling [18]. Therefore, MKPs exhibiting different subcellular localization and induction kinetics lead to strict spatio-temporal control of MAPKs.

MKPs are generally characterized as proteins degraded via the proteasome pathway and with a short half-life. Therefore, the actions of Bortezomib on endothelial cells expressing vGPCR can be mediated, at least in part, by the action of this drug on MAPKs through MKPs. Thus, the aim of this work was to further explore Bortezomib mechanism of action in vGPCR cells by investigating the role MKP-3 accumulation and ERK1/2 inhibition in this process.

## 2. Materials and methods

### 2.1. Chemicals and reagents

Bortezomib (S1013) was purchased in Selleck Chemicals (Nuclilab.nl, Rotterdam, NL). Immobilon P (polyvinylidene difluoride; PVDF) membranes were from Sigma-Aldrich (St. Louis, MO, USA). The antibodies used were: rabbit polyclonal anti-P-ERK1/2 (catalog no 4377), rabbit polyclonal anti-ERK1/2 (catalog no 9102), FOXO1 (catalog n$^{0}$ 2880), P-FOXO1 (catalog no 9461) from Cell Signaling (Cell Signaling Technology, Beverly, MA, USA), mouse anti-tubulin, mouse anti-MKP-3 (sc-166,041) as well as goat anti-rabbit - IgG-HRP (sc-2004), goat anti-mouse-IgG-HRP (sc-2005) antibodies from Santa Cruz Biotechnology (Santa Cruz, CA, USA). Anti- rabbit Cy2 (catalog no 111,225,144) was from Jackson (Jackson ImmunoResearch lab., West Grove, PA, USA) and DAPI (catalog n$^{0}$ D9542) from Sigma-Aldrich (St. Louis, MO, USA). PD 98059 was from Sigma-Aldrich (St. Louis, MO, USA). Protein A/G agarose were from Santa Cruz Biotechnology (Santa Cruz, CA, USA). PCR primers, Superscript III reverse transcriptase (Invitrogen), Sybr green PCR master mix (Applied Biosystems) were from Thermo Fisher (Thermo Fisher Scientific Inc., Waltham, MA, USA) Transfections were carried out using PolyFect (Qiagen, Valencia, CA, USA).

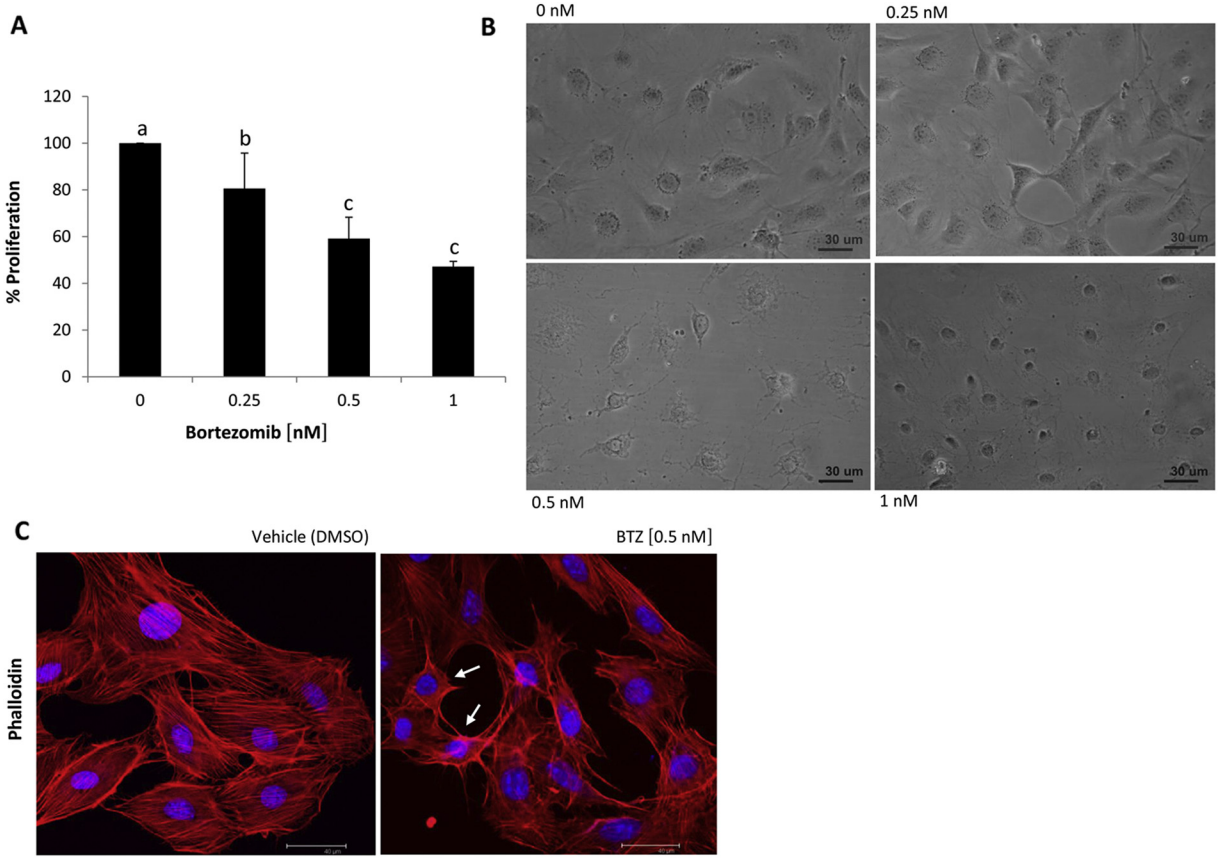


**Fig. 1.** Bortezomib decreases vGPCR cell number and induces cell morphology changes. Cells were serum starved for 24 h and then treated with 0.25–1 nM of Bortezomib or vehicle (DMSO) in DMEM 2% FBS for 24 h. Cells were then harvested and counted in a Neubauer chamber. A) Proliferation percentage was calculated between treated conditions and vehicle from four independent experiments. Percentage values (mean ± S.D.) were then represented in bar graphs. Significant differences between conditions were analyzed by one way ANOVA followed by Bonferroni test. Different letters indicate statistical differences among groups for each concentration ($p < 0.05$). B) In parallel, images from each concentration were taken in a phase contrast microscope and a representative micrograph is shown. Magnification 200×. C) Cells, treated with Bortezomib (0.5 nM, 24 h) or vehicle (DMSO), were fixed and incubated with anti-phalloidin (red) or DAPI (blue). Images were obtained by confocal microscopy and are representative of three independent experiments. Magnification 630×.

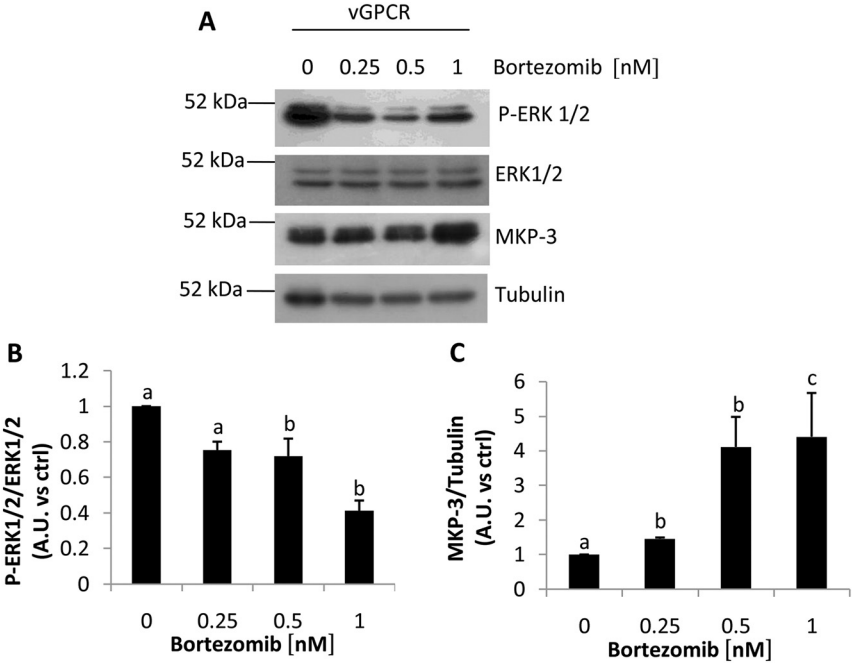


**Fig. 2.** Bortezomib reduces ERK1/2 phosphorylation and induces MKP-3 accumulation in a dose-dependent way. vGPCR cells were cultured and treated with 0.25–1 nM of Bortezomib or vehicle (DMSO) for 24 h. Cell lysates were prepared and subject to Western blot analysis with anti-P-ERK 1/2, Total ERK1/2, MKP-3 and Tubulin antibodies. A) A representative Western blot of at least 3 independent experiments is shown. Protein bands quantification from three independent experiments was done using Image J program. The results were then represented in bar graphs as a radio of P-ERK/Total ERK in B) or MKP-3/Tubulin in C) from each dose concentration versus the vehicle. Significant differences between vehicle and stimulated cells were analyzed by one way ANOVA followed by Bonferroni test, different letters indicate statistical differences among groups for each concentration ($p < 0.05$).

### 2.2. Cell lines, transfections and treatments

SV-40 immortalized murine endothelial cells stably expressing vGPCR full-length (vGPCR) were used [19]. Stable overexpression of vGPCR promotes tumor formation when these cells are injected into immuno-suppressed mice and induces angiogenic lesions similar to those developed in Kaposi Sarcoma [4,19]. Stable transfected cells were selected with 500 μg/ml G418 (Cellgro, Manassas, VA, USA).

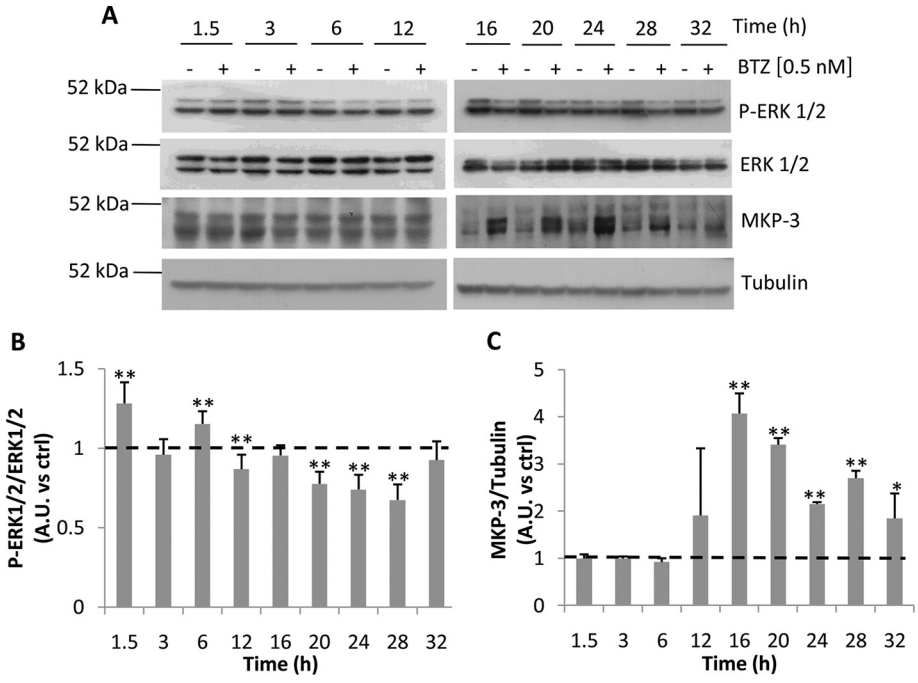


**Fig. 3.** Kinetic profile of P-ERK1/2 and MKP-3 induced by Bortezomib. Cells were cultured and treated with 0.5 nM of Bortezomib or vehicle (ctrl, DMSO) for 1.5–32 h. Cells lysates were prepared and subject to Western blot analysis with anti P-ERK1/2, Total ERK1/2, MKP-3 and Tubulin. A) Representative blots from at least three experiments are shown. Protein bands quantification by densitometry were when represented in bar graphs as the ratio between P-ERK1/2/Total ERK in B) and MKP-3/Tubulin in C) from control and treated conditions at each time point. Data analysis was done by Student's-test. $^{*}p < 0.05$, $^{**}p < 0.01$.

vGPCR endothelial cells were transfected with a shRNA against mouse MKP-3 (shMKP-3) designed by Dr. Paz'group [20]. MKP-3 knock-down was monitored by Western blot analysis. A recombinant plasmid encoding for MEK negative dominant MEKAA [21] was kindly provided by Dr. Alejandro Colman-Lerner (IFIBYNE Universidad de Buenos Aires - CONICET). MKP-3 knock-down and diminution of P-ERK1/2 was monitored by Western blot analysis. Plasmid transfections were done with PolyFect reagent following manufacturer's instructions (Qiagen). For all experiments, cells were grown in DMEM supplemented with 5% fetal bovine serum (FBS) and 500 μg/ml G418 to 80–90% confluence. Then, cells were starved for 24 h followed by Bortezomib (0.25–1 nM), inhibitor PD 98059 (10 μM) or control (vehicle, 0.1% DMSO) treatments carried out in 2% FBS medium. Cells were incubated under these conditions for the selected period of time.

### 2.3. Proliferation assays

vGPCR cells were seeded in 24-well plates, at 6000 cells per well. After overnight growth, the cells were starved for 24 h and then treated with Bortezomib (0.25–1 nM) or control (vehicle, 0.1% DMSO) in triplicate in DMEM-2% FBS for 24 h. Cells were then harvested and counted in a Neubauer chamber at the dose selected. Dead cells were excluded using tripan blue solution at 0.4%.

### 2.4. SDS- PAGE and Western blot analysis

For the preparation of total cell extracts, cells were scraped in 75 μl of lysis buffer containing: 50 mM Tris (pH 7.5), 150 mM NaCl, 0.1% Triton X-100, 1% Nonidet P-40, 2 mM EDTA, 2 mM EGTA, 25 mM β-glycerophosphate, 1 mM $Na_3VO_4$, 10 μg/ml leupeptin, 5 μg/ml aprotinin, 1 mM PMSF. Samples were incubated at 4 °C for 30 min, and centrifuged at 14,000*g* for 15 min. The supernatant was transfer to a new tube and protein concentration was measured by Bradford procedure [19]. Proteins from each experimental condition were resolved by SDS-PAGE and transferred to PVDF membranes and incubated with appropriately diluted specific primary antibodies after blocking unspecific sites on the membrane with 5% non-fat dry milk. Antibodies used include anti-p-ERK1/2 (1:1000), anti-ERK1/2 (1:1500), anti- MKP-3 (1:1500), anti-FOXO1 and p-FOXO1 (1:500), anti-tubulin (1:2000), combined with anti-rabbit (1:10,000) o anti-mouse (1:5000) horseradish peroxidase–conjugated secondary antibodies. Immunoreactive bands were detected by Amersham ECL Prime Western Blotting Detection Reagent (GE Healthcare, Little Chalfont, UK) and quantified using image J software, a public domain program, developed at the National Institutes of Health.

### 2.5. Phalloidin staining

vGPCR were cultured on cover slips and treated with 0.5 nM of Bortezomib or vehicle (0,1% DMSO). Then, cells were fixed in 4%

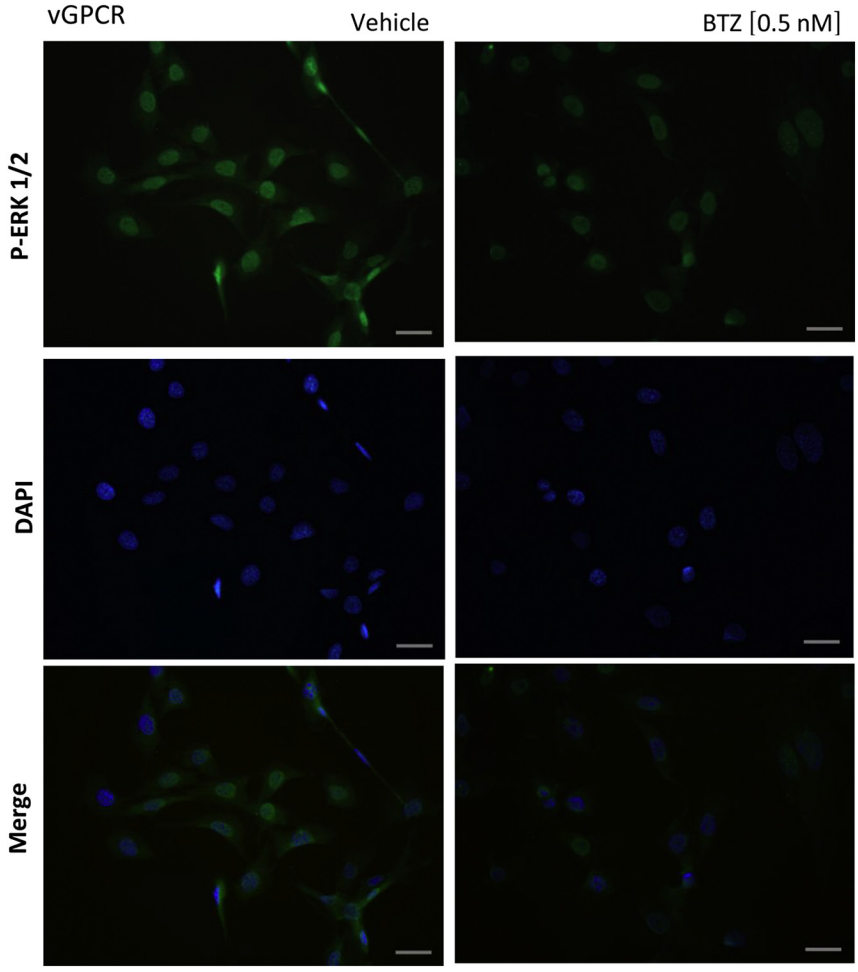


**Fig. 4.** Bortezomib decreases nuclear ERK1/2 phosphorylation. Cells treated with Bortezomib (0.5 nM, 24 h) were fixed with methanol (−20 °C) for 10 min. Then, cells were stained with anti-P-ERK1/2 (green) and DAPI (blue). Images representative of three independent experiments were obtained by a fluorescence microscope. Magnification 200×.

paraformaldehyde for 1 h and permeabilized in 0.1% Triton in PBS for 15 min, washed with PBS, and blocked with PBS 5% BSA for 30 min. Afterwards, the cells were incubated with anti-phalloidin conjugated with Rhodamine for 1 h at room temperature. After 3 washes with PBS (5 min), cells were incubated 5 min with DAPI. Images were taken with a Leica DM IRB2 microscope with a confocal spectral module SP2 equipped with Ar laser (458, 476, 488 and 514 nm) and HeNe laser (633 nm). Viewing was carried out with a 63 × 1.2 NA water-immersion objective.

### 2.6. Immunofluorescence microscopy

vGPCR cells were grown onto glass coverslips, starved and treated with or without Bortezomib (0.5 nM, 24 h). Then, cells were fixed with precooled methanol for 10 min at −20 °C, followed by two washes in PBS. For immunostaining, nonspecific sites were blocked with 5% BSA in PBS at room temperature for 30 min. Cells were incubated with the appropriate primary antibody (1:50 in PBS, 2% BSA, overnight at 4 °C). After three washes with PBS, cells were incubated with Cy-2-conjugated secondary antibody (1:200, 1 h, room temperature) and DAPI for nuclear staining. After washing with PBS at room temperature for 10 min, coverslips were mounted, and slides were viewed with an Olympus BX 5 fluorescence microscope.

### 2.7. Quantitative real-time PCR

Total RNA for quantitative reverse chain polymerase reaction (qRT-PCR) analysis was isolated by High Pure RNA Isolation Kit (Roche). 1 μg of RNA was reverse transcribed using the Superscript III Reverse transcriptase and qRT-PCR reactions were performed on the resulting cDNA (2 μl of cDNA; dilution 1/10) in a 7500 Fast Real Time PCR system (Applied Biosystems). Specific primers were used to detect VEGF, p21 levels and GAPDH to normalize gene expression. Oligonucleotides used for amplification were: murine *Vegfa*, forward, 5′-ATGAACTT TCTGCTCTCTTGGGTG-3′, and reverse, 5′-GACTTCTGCTCTCCTTCTGT CGTG-3′, murine *Gapdh*, forward, 5′-GAAGGTGAAGGTCGGAGTC-3′, and reverse, 5′-GAAGATGGTGATGGGATTTC-3′ [22]. For murine *p21*,

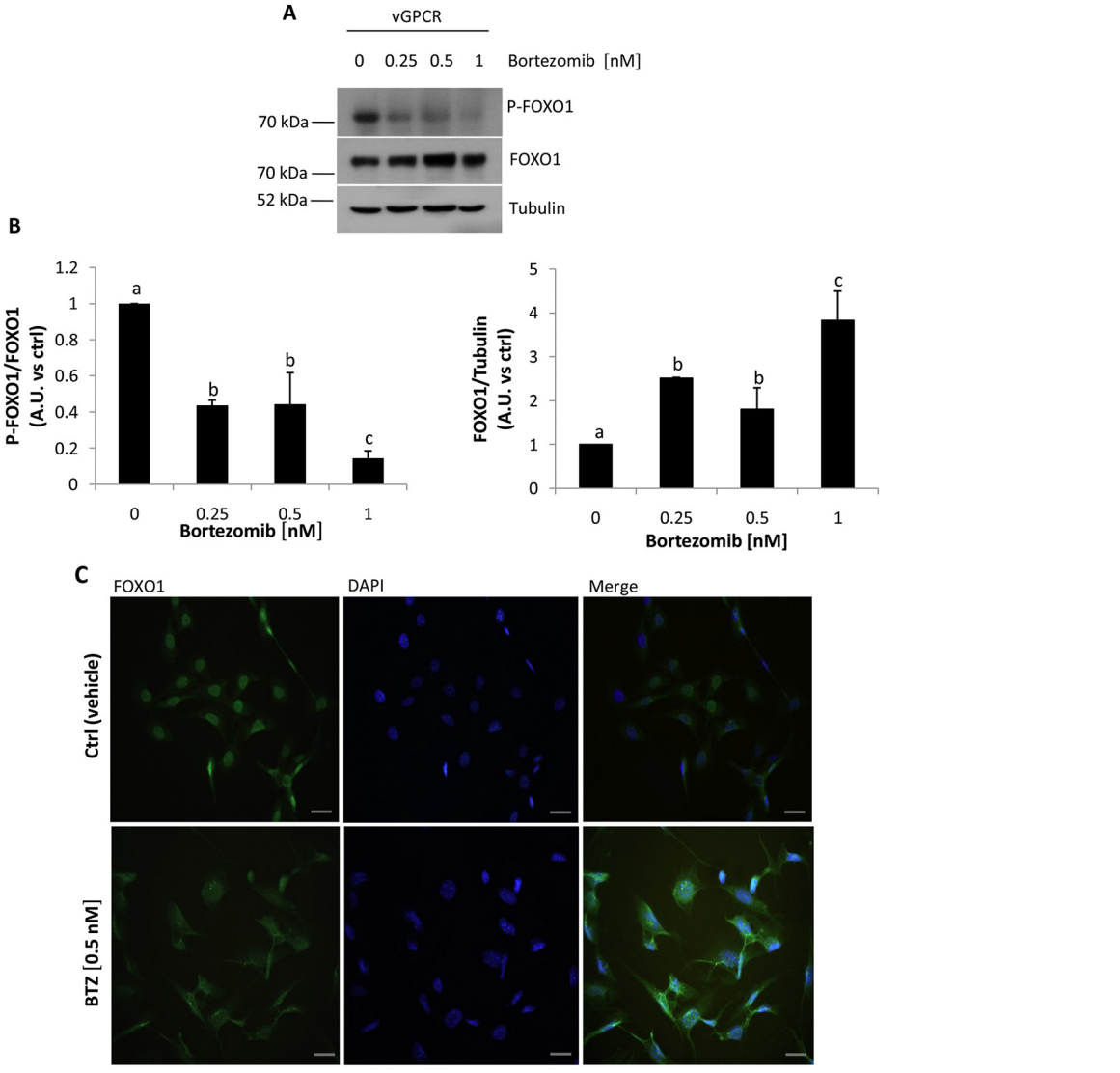


**Fig. 5.** Bortezomib increases FOXO1 levels and decreases FOXO1 phosphorylation. A) vGPCR cells were cultured and treated with 0.25–1 nM of Bortezomib or vehicle (DMSO) for 24 h. Cell lysates were prepared and subject to Western blot analysis with anti P-FOXO1, FOXO1 and Tubulin antibodies. A) Representative Western blots of three independent experiments are shown. B) Protein bands quantifications by densitometry were when represented in bar graphs as the ratio between P-FOXO1/FOXO1 (left panel) and FOXO1/Tubulin (right panel). Data analysis was done by ANOVA followed by Bonferroni test. Different letters indicate statistical differences among groups for each concentration ($p < 0.05$). C) Cells treated with Bortezomib (0.5 nM, 24 h) were fixed and stained with anti-FOXO1 (green) and DAPI (blue). Images representative of three independent experiments were obtained by a fluorescence microscope. Magnification 200×.

forward 5′-TTGGAGTCAG GCGCAGATCCACA-3′ and reverse 5′-CGCCATGAGCGCATCGCAATC-3′ [20].

### 2.8. Statistical analysis

Data are shown as means ± SD. Data from control and treated conditions obtained by qRT-PCR or Western blot were analyzed by the two-tailed *t*-test. *p* values < 0.01 (**) and <0.05 (*) were considered statistically significant. Data from dose response experiments obtained by qRT-PCR or Western blot were analyzed by one way ANOVA followed by Bonferroni test. Different superscript letters indicate significant differences at $^{*}p < 0.05$.

## 3. Results and discussion

### 3.1. Bortezomib decreases vGPCR cell growth

NF-κB is a transcription factor whose activation is required for many aspects of tumorigenesis, including cell growth and survival, angiogenesis, cell interaction and metastasis. In addition, proteasome inhibition has been shown to block chemotherapy-induced activation of NF-κB, resulting in enhanced chemosensitivity and increased apoptosis [8]. As Bortezomib induces cell cycle arrest in G0/G1 and decreases nuclear NF-κB activity in endothelial cells expressing vGPCR [13], we first investigated the effect of different doses of Bortezomib on vGPCR cell growth. To this end, cells were treated with Bortezomib (0.25–1 nM) in DMEM 2% FBS for 24 h and proliferation was analyzed by cell counting. As shown in Fig. 1, vGPCR cell proliferation decreased significantly in a dose-response manner, 0.5 and 1 nM being the most effective concentrations (Fig. 1A). In parallel, morphological changes observed by light field microscopy showed abnormal round cells and condensed nuclei (Fig. 1B). At molecular level, F-actin stained with phalloidin showed a regular array of defined actin filaments distributed in the cytoplasm of control vGPCR cells, and disorganized actin filaments, cytoplasm contraction and red fluorescence spots due to actin depolymerization in cells treated with 0.5 nM Bortezomib (Fig. 1C). Changes in actin cytoskeleton have been observed in other apoptotic cells. For instance, gypenoside, a natural compound from *Gynostemma pentaphyllum,* induces cell death and alterations in F-microfilaments in human colorectal SW-480 cells [23]. Also, dexamethasone has been shown to disrupt cytoskeleton organization and decrease the tumorigenicity of T47D human breast cancer cells [24].

### 3.2. Bortezomib modulates ERK1/2 phosphorylation and MKP-3 protein levels

ERK1/2 is highly activated in vGPCR cells [2]. Thus, the cell proliferation decrease promoted by Bortezomib can be attributed to an inhibition of ERK1/2 activity. Moreover, this drug could up-regulate MKP-3 levels leading to ERK inactivation. Thus, the next experiment evaluated the levels of MKP-3 and its substrate, phospho-ERK1/2 (P-ERK1/2), in vGPCR cells treated with Bortezomib (0.25–1 nM) for 24 h. As observed in Western blot analysis, Bortezomib induced a decrease in ERK1/2 phosphorylation but did not modify ERK1/2 protein levels (Fig. 2A). Data quantification indicates that the ratio P-ERK1/2/Total ERK1/2 decreased in a dose-dependent manner, an effect statistically significant at concentrations of 0.5 and 1 nM (Fig. 2B), whereas MKP-3 protein levels, normalized against tubulin levels, showed a concentration-dependent increase promoted by Bortezomib (0.5 and 1 nM) (Fig. 2C). Next, vGPCR cells were incubated in the presence or absence of Bortezomib (0.5 nM) for different times (1.5 to 32 h) in order to establish the kinetic profiles of P-ERK1/2 and MKP-3. Fig. 3A shows the results of a Western blot analysis evaluating P-ERK1/2 and MKP-3 levels. Data quantification revealed oscillations in P-ERK1/2 levels at short times of incubation with Bortezomib (1.5–16 h) (Fig. 3B). In contrast, a continuous decrease in P-ERK1/2 levels was detected after long times of incubation. Drug effect started at 20 h and remained statistically significant at 28 h (Fig. 3B). In parallel, MKP-3 protein levels increased significantly at 16 h and, although declining, remained high up to 32 h (Fig. 3C). The subcellular localization of phosphorylated ERK1/2 was evaluated by fluorescence microscopy in vGPCR cells treated for 24 h with Bortezomib (0.5 nM) or vehicle. Both experimental groups evidenced mostly nuclear localization of immunofluorescence, whereas Bortezomib-treated cells showed lower immunofluoresence intensity than vehicle-treated cells (Fig. 4). These results indicate that after 24 h the drug reduces P-ERK1/2 levels, in agreement with the results shown in Fig. 3A and B. And, as Bortezomib also produces MKP-3 accumulation, the decrease in P-ERK1/2 levels after long times of incubation may be mediated by MKP-3 rather than an inhibitory action on upstream ERK1/2 kinases. After a short period of incubation (1.5–16 h), Bortezomib did not significantly increase MKP-3 amount; however, in this period, significant variations were detected in P-ERK1/2 levels. As ERK1/2 is substrate of MKP-1 and MKP-2, dephosphorylation in this period could be produced by the action of these phosphatases. MKP-1 and MKP-2 are degraded by the proteasome pathway [15,25]. MKP-1, the product of an early gene, is rapidly translated and equally rapidly degraded, which leads to a transient increase in protein levels. Consistent

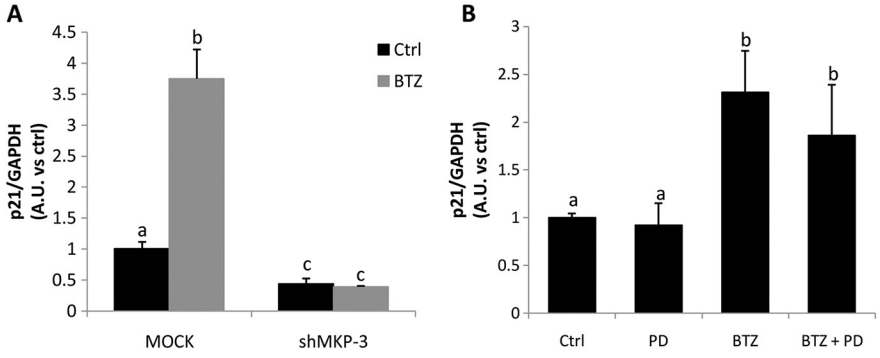


**Fig. 6.** Role of MKP-3 and ERK1/2 in Bortezomib-induced p21 expression. A) Cells were transfected with shRNA against MKP-3 or empty vector (MOCK) and treated with 0.5 nM of Bortezomib (BTZ) or vehicle (ctrl, DMSO). Total RNA was extracted and reverse transcribed and gene expression of p21 and GAPDH was assessed by qRT-PCR analysis at each condition. Bar graphs show quantitative results expressed as a ratio between each condition versus control MOCK samples normalized to GADPH mRNA levels B) Cells were incubated with 10 μM PD 98059 (PD) or transfected with MEKAA plasmid or equal amount of empty vector (Ctrl) or treated with 0.5 nM of Bortezomib (BTZ) for 24 h. Total RNA was extracted and reverse transcribed and data analysis was performed after by qRT-PCR. Bar graphs show quantitative results expressed as a ratio between each condition versus Ctrl normalized to GADPH mRNA levels. The statistical significance of the data from three independent experiments was done by ANOVA followed by Bonferroni test. Different letters indicate statistical differences among groups for each condition, $p < 0.05$).

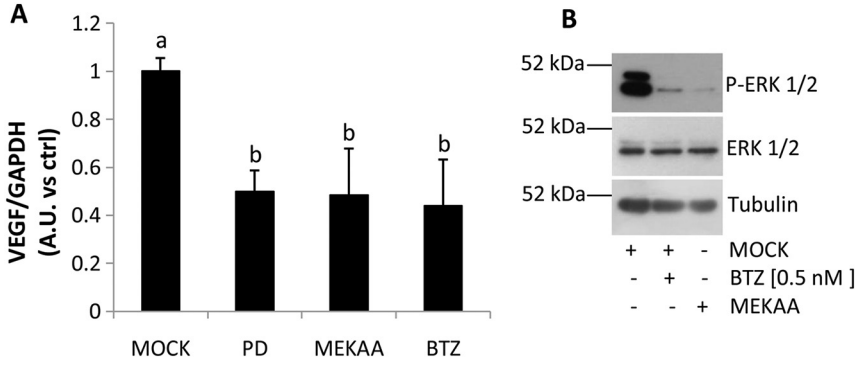


**Fig. 7.** Bortezomib inhibits VEGF expression through ERK1/2. vGPCR cells were cultured and transfected with MEKKAA or empty vector (MOCK) for 24 h, or incubated with PD98059 (10 μM, 24 h) or treated with of Bortezomib (0.5 nM, 24 h) or vehicle. A) Total RNA was extracted and reverse transcribed and gene expression of VEGF and GAPDH was assessed by qRT-PCR analysis. Data analysis was represented in bar graphs expressing the ratio between each condition versus control samples normalized to GADPH mRNA levels. The statistical significance of the data from three independent was analyzed by ANOVA followed by Bonferroni test. Different letters indicate statistical differences among groups for each condition ($p < 0.05$). B) Total cell lysates were analyzed by Western blot using anti-P-ERK1/2, Total ERK1/2 and Tubulin antibodies. Representative blots from three independent experiments are shown.

with this, it has been demonstrated that Bortezomib induces MKP-1 accumulation in MDA-MB-231 cells, an effect detected even at 4 h of incubation [26]. Taken together, an early and transient increase in MKP-1 followed by a similar increase in MKP-2 may explain the oscillations in P-ERK1/2 levels in the period 1.5–16 h.

### 3.3. Bortezomib regulates FOXO1 levels and activation

It has been shown that MKP-3 can also dephosphorylate a non-MAPK substrate, specifically the Forkhead box protein O1 (FOXO1), promoting its nuclear localization and activation of key gluconeogenic genes [27,28]. Thus, the next experiments tested whether Bortezomib, by its accumulative effect on MKP-3, regulates FOXO1 phosphorylation state (Fig. 5). Western blot analysis revealed a concentration-dependent decrease in P-FOXO1 and an increase in FOXO1, which rendered a decrease in the ratio P-FOXO1/FOXO1 after 24 h of cell treatment (Fig. 5B, left panel) and an increase in the ratio FOXO1/Tubulin (Fig. 5B, right panel). The increase in total FOXO1 may be explained by its degradation through the proteasome pathway [29,30]; therefore this transcription factor is expectably up-regulated by Bortezomib. On the other hand, the fact that Bortezomib reduces P-FOXO1/total FOXO1 but increases total FOXO1/Tubulin suggests that this drug is capable of regulating FOXO1 protein at two levels, promoting both its expression and its dephosphorylation.

We have also analyzed FOXO1 localization by fluorescence microscopy (Fig. 5C) following the procedures described for Fig. 4. In basal conditions, FOXO1 signal was dim and diffuse in both nucleus and cytosol compartments. After Bortezomib treatment (0.5 nM, 24 h) FOXO1 signal increased and mostly concentrated in the nucleus. These results showing that Bortezomib induces the accumulation of FOXO1 in the nucleus reinforce the notion that this drug promotes FOXO1 dephosphorylation and activation.

It has been recently demonstrated that dexamethasone, a synthetic glucocorticoid, increases MKP-3 protein expression both in cultured hepatoma cells and in mouse liver through a mechanism that requires FOXO1 activation. Moreover, the overexpression of FOXO1 is sufficient to induce MKP-3 protein expression [31]. Then, our findings depict a model of Bortezomib action including the accumulation of both MKP-3 and FOXO1 as a consequence of proteasome inhibition and the induction of MKP-3, probably as a consequence of FOXO1 activation.

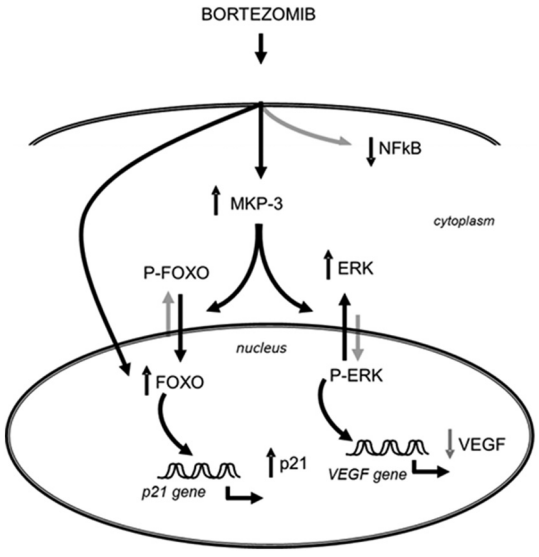


**Fig. 8.** Proposed model for Bortezomib action on vGPCR cells. Bortezomib triggers MKP-3 accumulation. The activity of this phosphatase reduces P-ERK and P-FOXO1 levels, which renders ERK1/2 deactivation and FOXO1 activation, respectively. While ERK deactivation reduces VEGF expression, FOXO1 activation promotes p21 induction. All these events converge in the inhibition of cell proliferation.

### 3.4. p21 is induced by Bortezomib in a MKP-3-dependent way

Increasing evidence indicates that FOXO1 is necessary for the transcription of the cell cycle inhibitor p21 [20,32,33]. Since MKP-3 participates in the dephosphorylation and activation of P-FOXO1 [28], variations in MKP-3 levels produced by Bortezomib could influence p21 expression. In addition, MKP-3 promotes ERK1/2 dephosphorylation, an effect which could also impact p21 expression. Indeed, the role of ERK 1/2 in the expression of p21 in vGPCR cells has not been determined yet. Thus, we investigated whether Bortezomib increases p21 mRNA levels and whether MKP-3 and/or ERK1/2 inhibition participate in this event. For this, vGPCR cells were plated and transfected with a plasmid for the expression of a shMKP-3 mRNA [20] or the empty vector (Mock) incubated with Bortezomib (BTZ, 0.5 nM) or vehicle (Ctrl) and processed in order to evaluate the mRNA levels of p21 and GAPDH as loading control. In other experiments, p21 mRNA levels were evaluated in cells incubated with vehicle (Ctrl), Bortezomib (BTZ, 0.5 nM) or PD 98059 (PD, 10 μM), an inhibitor of ERK1/2 upstream kinases - that is MEK1/2 - which reduces ERK1/2 phosphorylation and activation As shown in Fig. 6A, Bortezomib significantly increased p21 mRNA levels, an effect which was blocked when MKP-3 was knocked down by the specific shRNA. It should be noted that MKP-3 down regulation also reduced the basal levels of p21 mRNA. These results indicate that MKP-3 is necessary for p21 expression, although whether it is required for the dephosphorylation of P-ERK1/2 or P-FOXO1 remains undetermined. The

fact that PD 98059 did not reduce p21 mRNA levels (Fig. 6B) suggests that P-ERK dephosphorylation is not involved in basal or Bortezomib-induced p21 upregulation. Therefore, MKP-3 activity is likely to be required for P-FOXO1 dephosphorylation rather than for P-ERK dephosphorylation.

Our findings indicate that Bortezomib-induced p21 expression in vGPCR cells does not involved MEK/ERK pathway. Nevertheless, the role of this pathway in the regulation of p21 seems to be stimulus- and cell-specific. For example, antifungal drug terbinafine (TB) decreases the levels of P-ERK and induces both the upregulation of p21 and cell cycle arrest in cultured human umbilical vein endothelial cells, which suggests that p21 up regulation is dependent on ERK dephosphorylation [34]. In contrast, tumor promoter 12-O-tetradecanoylphorbol-13-acetate (TPA) increases the level of p21 expression in breast cancer cell lines MCF-7 and MDA-MB-231, an effect blocked by a MEK1/2 inhibitor. This results indicates that TPA-induced upregulation of p21 requires ERK phosphorylation [35]. Taken together, these studies reveal that Bortezomib can induce cell cycle inhibitor p21, probably through a mechanism involving MKP-3-mediated FOXO1 dephosphorylation.

### *3.5. Bortezomib inhibits VEGF expression by inhibition of ERK1/2 phosphorylation*

vGPCR transforming effect involves the activation of MAPKs and small GTPases whose activities converge in the nucleus to control transcription factors, thereby promoting the expression and secretion of VEGF and pro-inflammatory cytokines [2]. The next experiments were then meant to determine whether VEGF expression is dependent on ERK1/2 activity and hence likely to be targeted by Bortezomib.

VEGF mRNA was thus evaluated in non-treated cells and in cells treated to downregulate ERK activity by three different approaches:1-incubation with PD98059 (10 μM); 2-transfection with a plasmid for the expression of MEKAA, a negative dominant form of MEK which impairs ERK1/2 phosphorylation; 3-incubation with Bortezomib (0.5 nM). Cells were transfected with a MEKAA-encoding vector and then incubated with vehicle (MEKAA) or transfected with the empty vector and then incubated with vehicle (Mock), Bortezomib (BTZ) or PD 98059 (PD). After treatment, cells were processed and VEGF and GAPDH mRNA levels were evaluated. As shown in Fig. 7A, VEGF was expressed in untreated vGPCR cells and its expression levels were significantly lower upon PD 98059 treatment or MEKAA expression. Bortezomib treatment also reduced VEGF expression in a magnitude similar to those of MEK inhibitor treatment or MEKAA expression. These results suggest that ERK activity has a critical role in VEGF expression in vGPCR-transformed cells. As a consequence, Bortezomib may be expected to have similar effects, as it is capable of promoting ERK1/2 dephosphorylation through MKP-3 induction. Indeed, P-ERK 1/2 levels were barely detected after 24 h of Bortezomib treatment or MEKAA expression but exhibited strong signal in vehicle-treated cells, which indicates high P-ERK1/2 levels (Fig. 7B). These results confirm the role of ERK1/2 in VEGF expression, as described in other cellular types [36,37]. As Bortezomib reduces VEGF expression, probably promoting ERK dephosphorylation through MKP-3, VEGF may be considered its additional target.

Our results showing in vitro actions of Bortezomib on several points of cellular biology suggest that it could interfere in vivo with tumor development in different ways. Bortezomib is currently approved for the treatment of multiple myeloma (MM) [38]. In addition to its general mechanism through proteasome inhibition, Bortezomib counteracts myeloma by inhibiting NF-κB transcriptional activity [39]. NF-κB has been shown to be constitutively activated in several types of cancer cells, and its blockade has been reported to increase cell susceptibility to apoptosis [40]. Therefore, the use of this drug to increase cell apoptosis in other cancer in addition to MM seems feasible. Indeed, Bortezomib down-regulates the migration and invasion of hepatocellular carcinoma (HCC) cells by suppressing focal adhesion kinase expression through a mechanism involving NF-κB [41]. However, the use of Bortezomib alone has been proven inefficient as a single-agent therapy in unresectable HCC patients [42], although dual therapies including Bortezomib remain possible. Indeed, several studies suggest that Bortezomib may have an additive antitumoral activity in combined treatments in vitro [43,44] as well as in vivo [45]. Even to treat patients with relapsed/refractory MM, treatment with Bortezomib and melphalan [46] or thalidomide [47] has been successfully used. As we have previously demonstrated that both vitamin D analog TX 527 [13] and its parental hormone $1\alpha,25(OH)_2$ vitamin $D_3$ inhibit NF-κB pathway [48] inducing apoptosis in vGPCR cells [49], an approach combining Bortezomib and some of these agents may prove beneficial in the treatment of Kaposi's sarcoma disease. Nevertheless, studies should be carried out in animal models for further experimental support.

In conclusion, we demonstrate that Bortezomib inhibits vGPCR cell growth by accumulation of MKP-3. The activity of this phosphatase reduces P-ERK and P-FOXO1 levels, which renders ERK1/2 deactivation and FOXO1 activation, respectively. While ERK deactivation reduces VEGF expression, FOXO1 activation promotes p21 induction. As depicted in Fig. 8, Bortezomib triggers MKP-3 accumulation in vGPCR cells, which promotes ERK and FOXO1 dephosphorylation, FOXO1-dependent p21 induction and also the inhibition of VEGF expression. All these events converge in the inhibition of cell proliferation.

## Acknowledgments

This work was supported by grants from Agencia Nacional de Promoción Científica y Tecnológica (ANPCYT, PICT 2013-0562 to VGP and PICT 2014-1006 to CP), Consejo Nacional de Investigaciones Científicas y Tecnológicas (CONICET, PIP1122011010040 to VGP and PIP 11220110100101 to CP, Universidad Nacional del Sur to VGP (PGI 24/B188) and Universidad de Buenos Aires to CP (2002 0130100300). We also wish to thank Dr. by Dr. Alejandro Colman-Lerner (IFIBYNE Universidad de Buenos Aires - CONICET) for providing MEKAA plasmid.

## References

[1] Y. Chang, E. Cesarman, M.S. Pessin, F. Lee, J. Culpepper, D.M. Knowles, P.S. Moore, Identification of herpesvirus-like DNA sequences in AIDS-associated Kaposi's sarcoma, Science 266 (1994) 1865–1869.
[2] D. Martin, J.S. Gutkind, Human tumor-associated viruses and new insight into the molecular mechanisms of cancer, Oncogene 27 (2009) S31–S42.
[3] E.A. Mesri, E. Cesarman, C. Boshoff, Kaposi's sarcoma and its associated herpesvirus, Nat. Rev. Cancer 10 (2010) 707–719.
[4] S. Montaner, A. Sodhi, A. Molinolo, T.H. Bugge, E.T. Sawai, Y. He, Y. Li, P.E. Ray, J.S. Gutkind, Endothelial infection with KSHV genes in vivo reveals that vGPCR initiates Kaposi's sarcomagenesis and can promote the tumorigenic potential of viral latent genes, Cancer Cell 3 (2003) 23–26.
[5] M.G. Grisotto, A. Garin, A.P. Martin, K.K. Jensen, P. Chan, S.C. Sealfon, S.A. Lira, The human herpesvirus 8 chemokine receptor vGPCR triggers autonomous proliferation of endothelial cells, J. Clin. Invest. 116 (2006) 1264–1273.
[6] S. Montaner, A. Sodhi, A.K. Ramsdell, D. Martin, J. Hu, E.T. Sawai, J.S. Gutkind, The Kaposi's sarcoma-associated herpesvirus G protein-coupled receptor as a therapeutic target for the treatment of Kaposi's sarcoma, Cancer Res. 66 (2006) 168–174.
[7] D. Martin, R. Galisteo, Y. Ji, S. Montaner, J.S. Gutkind, An NF-κB gene expression signature contributes to Kaposi's sarcoma virus vGPCR-induced direct and paracrine neoplasia, Oncogene 27 (2008) 1844–1852.
[8] J. Adams, M. Kauffman, Development of the proteasome inhibitor Velcade (bortezomib), Cancer Investig. 22 (2004) 304–311.
[9] C. Blackburn, K.M. Gigstad, P. Hales, K. Garcia, M. Jones, F. Bruzzese, C. Barrett, J.X. Liu, T.A. Soucy, D.S. Sappal, N. Bump, E.J. Olhava, P. Fleming, L.R. Dick, C. Tsu, M.D. Sintchak, J.J.L. Blank, Characterization of a new series of non-covalent proteasome inhibitors with exquisite potency and selectivity for the 20S β5-subunit, Biochem. J. 430 (2010) 461–476.
[10] J. Adams, V.J. Palombella, E.A. Sausville, J. Johnson, A. Destree, D.D. Lazarus, J. Maas, C.S. Pien, S. Prakash, P.J. Elliott, Proteasome inhibitors: a novel class of potent and effective antitumor agents, Cancer Res. 59 (1999) 2615–2622.
[11] T. Hideshima, P. Richardson, D. Chauhan, V.J. Palombella, P.J. Elliott, J. Adams, K.C. Anderson, The proteasome inhibitor PS-341 inhibits growth, induces apoptosis, and overcomes drug resistance in human multiple myeloma cells, Cancer Res. 61 (2001) 3071–3076.
[12] C. Kao, A. Chao, C.L. Tsai, C.Y. Lin, W.C. Chuang, H.W. Chen, T.C. Yen, T.H. Wang, C.H. Lai, H.S. Wang, Phosphorylation of signal transducer and activator of transcription 1

reduces bortezomib-mediated apoptosis in cancer cells, Cell Death Dis. 4 (2013), e512.
[13] V. González-Pardo, A. Verstuyf, R. Boland, A. Russo de Boland, Vitamin D analogue TX 527 down-regulates the NF-κB pathway and controls the proliferation of endothelial cells transformed by Kaposi sarcoma herpesvirus, Br. J. Pharmacol. 169 (2013) 1635–1645.
[14] A. Suares, A. Russo de Boland, A. Verstuyf, R. Boland, V. González-Pardo, The proapoptotic protein Bim is up regulated by 1α,25-dihydroxyvitamin D3 and its receptor agonist in endothelial cells and transformed by viral GPCR associated to Kaposi sarcoma, Steroids 102 (2015) 85–91.
[15] T. Boutros, E. Chevet, P. Metrakos, Mitogen-activated protein (MAP) kinase/MAP kinase phosphatase regulation: roles in cell growth, death, and cancer, Pharmacol. Rev. 60 (2008) 261–310.
[16] C.Y. Huang, T.H. Tan, DUSPs, to MAP kinases and beyond, Cell Biosci. 2 (2012) 24.
[17] C.J. Caunt, S.M. Keyse, Dual-specificity MAP kinase phosphatases (MKPs): shaping the outcome of MAP kinase signaling, FEBS J. 280 (2013) 489–504.
[18] Y. Zhao, Z.Y. Zhang, The mechanism of dephosphorylation of extracellular signal-regulated kinase 2 by mitogen-activated protein kinase phosphatase 3, J. Biol. Chem. 276 (2001) 32382–32391.
[19] V. González Pardo, D. Martin, J.S. Gutkind, A. Verstuyf, R. Bouillon, A. Russo de Boland, R. Boland, 1alpha,25-dihydroxyvitamin D3 and its TX527 analog inhibit the growth of endothelial cells transformed by Kaposi sarcoma-associated herpes virus G protein-coupled receptor in vitro and in vivo, Endocrinology 151 (2010) 23–31.
[20] M. Mori Sequeiros García, N.V. Gómez, A. Gorostizaga, A. Acquier, S.I. González-Calvar, C.F. Mendez, C. Paz, MAP kinase phosphatase-3 (MKP-3) is transcriptionally and post-translationally up-regulated by hCG and modulates cAMP-induced p21 expression in MA-10 Leydig cells, Mol. Cell. Endocrinol. 371 (2013) 174–181.
[21] M.J. Marinissen, M. Chiariello, M. Pallante, J.S. Gutkind, A network of mitogen-activated protein kinases links G protein-coupled receptors to the c-Jun promoter: a role for c-Jun NH2-terminal kinase, p38s, and extracellular signal-regulated kinase 5, Mol. Cell. Biol. 19 (1999) 4289–4301.
[22] D. Martin, R. Galisteo, J.S. Gutkind, CXCL8/IL8 stimulates vascular endothelial growth factor (VEGF) expression and the autocrine activation of VEGFR2 in endothelial cells by activating NFkappaB through the CBM (Carma3/Bcl10/Malt1) complex, J. Biol. Chem. 284 (2009) 6038–6042.
[23] H. Yan, X. Wang, J. Niu, Y. Wang, P. Wang, Q. Liu, Anti-cancer effect and the underlying mechanisms of gypenosides on human colorectal cancer SW-480 cells, PLoS One 9 (2014), e95609.
[24] X.G. Meng, S.W. Yue, Dexamethasone disrupts cytoskeleton organization and migration of T47D human breast cancer cells by modulating the AKT/mTOR/RhoA pathway, Asian Pac. J. Cancer Prev. 15 (2014) 10245–10250.
[25] D.J. Peng, J.Y. Zhou, G.S. Wu, Post-translational regulation of mitogen-activated protein kinase phosphatase-2 (MKP-2) by ERK, Cell Cycle 9 (2010) 4650–4655.
[26] B.S. Patel, W.S. Co, C. Donat, M. Wang, W. Che, P. Prabhala, F. Schuster, V. Schulz, J.L. Martin, A.J. Ammit, Repression of breast cancer cell growth by proteasome inhibitors in vitro: impact of mitogen-activated protein kinase phosphatase 1, Cancer Biol. Ther. 16 (2015) 780–789.
[27] P. Jiao, B. Feng, H. Xu, Mapping MKP-3/FOXO1 interaction and evaluating the effect on gluconeogenesis, PLoS One 7 (2012), e41168.
[28] Z. Wu, P. Jiao, X. Huang, B. Feng, Y. Feng, S. Yang, P. Hwang, J. Du, Y. Nie, G. Xiao, H. Xu, MAPK phosphatase-3 promotes hepatic gluconeogenesis through dephosphorylation of forkhead box O1 in mice, J. Clin. Invest. 120 (2010) 3901–3911.
[29] Y. Iwaihara, S. Ishikura, K. Doi, T. Tsunoda, T. Fujimoto, T. Okamura, S. Shirasawa, Marked reduction in FoxO1 protein by its enhanced proteasomal degradation in Z fat-deficient peripheral T-cells, Anticancer Res. 35 (2015) 4419–4423.
[30] H. Jang, G.Y. Lee, C.P. Selby, G. Lee, Y.G. Jeon, J.H. Lee, K.K. Cheng, P. Titchenell, M.J. Birnbaum, A. Xu, A. Sancar, J.B. Kim, SREBP1c-CRY1 signalling represses hepatic glucose production by promoting FOXO1 degradation during refeeding, Nat. Commun. 7 (2016) 12180.
[31] B. Feng, Q. He, H. Xu, FOXO1-dependent up-regulation of MAP kinase phosphatase 3 (MKP-3) mediates glucocorticoid-induced hepatic lipid accumulation in mice, Mol. Cell. Endocrinol. 393 (2014) 46–55.
[32] S.K. Roy, R.K. Srivastava, S. Shankar, Inhibition of PI3K/AKT and MAPK/ERK pathways causes activation of FOXO transcription factor, leading to cell cycle arrest and apoptosis in pancreatic cancer, J. Mol. Signal. (2010).
[33] D.E. Kloet, P.E. Polderman, A. Eijkelenboom, L.M. Smits, M.H. van Triest, M.C. van den Berg, M.J. Groot Koerkamp, D. van Leenen, P. Lijnzaad, F.C. Holstege, B.M. Burgering, FOXO target gene CTDSP2 regulates cell cycle progression through Ras and p21(Cip1/Waf1), Biochem. J. 469 (2015) 289–298.
[34] P.Y. Ho, S.P. Hsu, Y.C. Liang, M.L. Kuo, Y.S. Ho, W.S. Lee, Inhibition of the ERK phosphorylation plays a role in terbinafine-induced p21 up-regulation and DNA synthesis inhibition in human vascular endothelial cells, Toxicol. Appl. Pharmacol. 229 (2008) 86–93.
[35] J. Han, S. Kim, J.H. Yang, S.J. Nam, J.E. Lee, TPA-induced p21 expression augments G2/M arrest through a p53-independent mechanism in human breast cancer cells, Oncol. Rep. 27 (2012) 517–522.
[36] J. Wang, C. He, T. Zhou, Z. Huang, L. Zhou, X. Liu, NGF increases VEGF expression and promotes cell proliferation via ERK1/2 and AKT signaling in Müller cells, Mol. Vis. 22 (2016) 254–2063 (eCollection 2016).
[37] J. Xu, Y. Yi, L. Li, W. Zhang, J. Wang, Osteopontin induces vascular endothelial growth factor expression in articular cartilage through PI3K/AKT and ERK1/2 signaling, Mol. Med. Rep. 12 (2015) 4708–4712.
[38] P.G. Richardson, B. Barlogie, J. Berenson, S. Singhal, S. Jagannath, D. Irwin, S.V. Rajkumar, G. Srkalovic, M. Alsina, R. Alexanian, D. Siegel, R.Z. Orlowski, D. Kuter, S.A. Limentani, S. Lee, T. Hideshima, D.L. Esseltine, M. Kauffman, J. Adams, D.P. Schenkein, K.C. Anderson, A phase 2 study of bortezomib in relapsed, refractory myeloma, N. Engl. J. Med. 348 (2003) 2609–2617.
[39] A. Paramore, S. Frantz, Bortezomib, Nat. Rev. Drug Discov. 2 (2003) 611–612.
[40] Y. Xia, S. Shen, I.M. Verma, NF-κB, an active player in human cancers, Cancer Immunol. Res. 2 (2014) 823–830.
[41] B.S. Ko, T.C. Chang, C.H. Chen, C.C. Liu, C.C. Kuo, C. Hsu, Y.C. Shen, T.L. Shen, V.M. Golubovskaya, C.C. Chang, S.K. Shyue, J.Y. Liou, Bortezomib suppresses focal adhesion kinase expression via interrupting nuclear factor kappa B, Life Sci. 86 (2010) 199–206.
[42] G.P. Kim, M.R. Mahoney, D. Szydlo, T.S. Mok, R. Marshke, K. Holen, J. Picus, M. Boyer, H.C. Pitot, J. Rubin, P.A. Philip, A. Nowak, J.J. Wright, C. Erlichman, An international, multicenter phase II trial of bortezomib in patients with hepatocellular carcinoma, Investig. New Drugs 30 (2012) 387–394.
[43] C. Wang, D. Gao, K. Guo, X. Kang, K. Jiang, C. Sun, Y. Li, L. Sun, H. Shu, G. Jin, H. Sun, W. Wu, Y. Liu, Novel synergistic antitumor effects of rapamycin with bortezomib on hepatocellular carcinoma cells and orthotopic tumor model, BMC Cancer 12 (2012) 166.
[44] M. Maynadier, I. Basile, A. Gallud, M. Gary-Bobo, M. Garcia, Combination treatment with proteasome inhibitors and antiestrogens has a synergistic effect mediated by p21WAF1 in estrogen receptor-positive breast cancer, Oncol. Rep. 36 (2016) 1127–1134.
[45] G.S. Falchook, J.J. Wheler, A. Naing, E.F. Jackson, F. Janku, D. Hong, C.S. Ng, N.M. Tannir, K.N. Lawhorn, M. Huang, L.S. Angelo, D. Vishwamitra, K. Hess, A.N. Howard, K.L. Parkhurst, H.M. Amin, R. Kurzrock, Oncotarget 5 (2014) 10280–10292.
[46] J.R. Berenson, H.H. Yang, K. Sadler, S.G. Jarutirasarn, R.A. Vescio, R. Mapes, M. Purner, S.P. Lee, J. Wilson, B. Morrison, J. Adams, D. Schenkein, R. Swift, Phase I/II trial assessing bortezomib and melphalan combination therapy for the treatment of patients with relapsed or refractory multiple myeloma, J. Clin. Oncol. 24 (2006) 937–944.
[47] B. Barlogie, J. Shaughnessy, G. Tricot, J. Jacobson, M. Zangari, E. Anaissie, R. Walker, J. Crowley, Treatment of multiple myeloma, Blood 103 (2004) 20–32.
[48] V. González Pardo, N. D'Elia, A. Verstuyf, R. Boland, A. Russo de Boland, NF-κB pathway is down-regulated by 1α25(OH)2-vitamin D3 in endothelial cells transformed by Kaposi sarcoma-associated herpesvirus G protein coupled receptor, Steroids 77 (2012) 1025–1032.
[49] V. González Pardo, A. Suares, A. Verstuyf, P. De Clercq, R. Boland, A. Russo de Boland, Cell cycle arrest and apoptosis induced by 1α,25(OH)2D3 and TX527 in Kaposi sarcoma is VDR dependent, J. Steroid Biochem. Mol. Biol. 144 (2014) 197–200.